

# Multiport Converter Topology for Hybrid System Using PI Controllers

Ms Reshmi Ravi K<sup>1</sup>, Mrs Renu Jose<sup>2</sup>

Power Electronics, Electrical and Electronics Department, TocH Institute of Science and Technology,  
Arakkunnam, Ernakulam, Kerala, India

**Abstract:** Renewable energy sources such as Fuel-Cells, Photo-Voltaic (PV) arrays are increasingly using in automobiles, residential and commercial buildings. For stand-alone systems energy storage devices are required for backup power and fast dynamic response. A power electronic converter interfaces the sources with the load along with energy storage. Existing converters for such applications use a common dc-link, which employ multiple converters. Proposed system in this paper is a systematic method for deriving three-port converters (TPCs) from the full-bridge converter (FBC). The three port converter features single stage conversion between any two of the three ports, higher system efficiency, fewer components, faster response and compact packaging. The proposed FB-TPC consists of two bidirectional ports and an isolated output port. The primary circuit of the converter functions as a buck-boost converter and provides a power flow path between the ports on the primary side. The FB-TPC can adapt to a wide source voltage range. Here MATLAB using Simulink and SimPower System set toolboxes is used for software implementation.

**Key words:** Photo-Voltaic (PV), Boost-buck, dc-dc converter, full-bridge converter (FBC), renewable power system, three-port converter (TPC)

## I. INTRODUCTION

Renewable energy sources such as fuel cells, photovoltaic (PV) arrays are widely used in automobiles, residential and commercial buildings. They are intermittent in nature. Energy storage devices are needed for backup power for stand-alone systems. A converter is required to interface renewable resources, storage and loads. Recently three port converters are gaining more attention than conventional converters.

In the conventional structure [3]-[4] a common high-voltage or low-voltage DC bus is used to interconnect multiple sources which requires several conversion stages. Drawback of this structure is inherently complex and has a high cost due to the multiple conversion stages and communication devices between individual converters. As shown in Fig 1, it proposes a multiport structure. Compared to the conventional one, in the proposed structure the whole system is treated as a single power converter, which combines multiple sources.

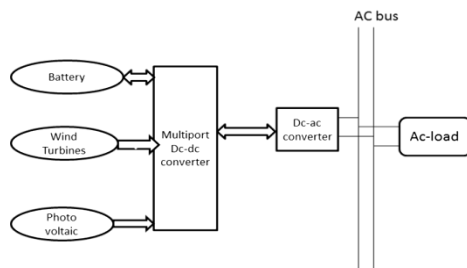


Figure 1-Block diagram of the multi-port structure

Generally, the multiport converters (MPCs) can be classified into three categories:

- Fully isolated topologies
- Fully non-isolated topologies and
- Partly isolated topologies.

Fully isolated MPCs [12],[15],[16] are derived by combining full-bridge, half-bridge or series-resonant topologies via magnetic coupling. In these topologies isolation, bidirectional capabilities of all the ports and zero-voltage-switching (ZVS) can be achieved. These MPCs are good for the applications where isolation and bidirectional conversion are required. But, the major problem is that too many active switches are used which results in complicated driving and control circuitry. This results in degradation of the reliability and performance of the integrated converters.

Non-isolated MPCs [17],[18] can either be derived by using integration method or DC-link. These MPCs provide compact design and high-power density. But voltage levels of all ports are not flexible and ZVS cannot be achieved easily.

Partly isolated MPCs [3],[7],[19],[20] are hybrid topologies of isolated circuits and non-isolated circuits, which can provide necessary isolation for the load and maintain advantages of compact design and high power density. This paper is organized as follows. In section II discusses about the proposed topology and section IV explains the control strategy. Simulation results are presented in section V, to

verify the proposed method. Finally, conclusions and future scope will be given in VI and VII.

## II. PROPOSED THREE PORT CONVERTER TOPOLOGY

A three-port energy management system includes a primary source and storage, and, single-stage power conversion between any two of the three ports is possible. Having the two energy inputs, the instantaneous power can be redistributed in the system in a controlled manner, which results in improvement of system dynamics and reliability. Another advantage of using a three-port system is that the primary source only needs to be sized according to the average power consumed by the load, not necessarily to the peak power. This operation is economically beneficial since per watt cost of the primary source is usually high, and thus it makes sense to operate the primary source at the maximum power.

### A. Circuit and topology

This chapter refers to a three-port converter using a single-stage power conversion is proposed and analyzed. Here a suitable method for generating TPC topologies from full bridge converters and to find a novel full-bridge TPC with single-stage power conversion between any two of the three ports. A buck-boost converter is integrated in the proposed FB-TPC, it can adapt to applications with a wide source voltage range. ZVS of all the primary-side switches can also be obtained with the proposed FB-TPC.

In the Fig.2(a), the primary side of the FBC consists of two switching legs, composed of  $S_{A1}$ ,  $S_{A2}$  and  $S_{B1}$ ,  $S_{B2}$ , in parallel, connected to a common input source  $V_s$ . The voltage-second balance principle of the magnetizing inductor  $L_m$  is the constraint condition of the operation of the FBC in the primary side. This means that, the two switching legs of the FBC can be split into two symmetrical parts, cells A and B, if only  $L_m$  satisfies the voltage-second balance principle, as shown in Fig.2(b). The two cells can be directly connected to different sources,  $V_{sa}$  and  $V_{sb}$ , respectively, as shown in Fig.2(c), and then a novel FB-TPC is derived.

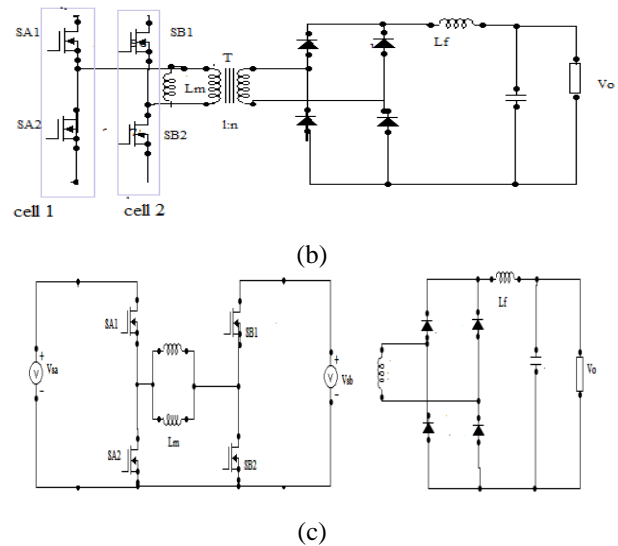


Fig 2-Proposed derivation of full-bridge three-port converter (a) Full-bridge Converter (b) Two-switching cells (c) Full-bridge three-port converter

## III. SWITCHING STATE ANALYSIS

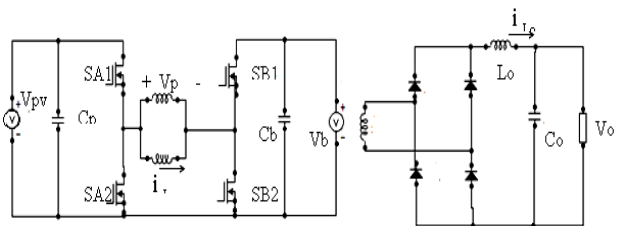


Fig. 3 Topology of the proposed FB-TPC

To verify the proposed topology the FB-TPC, is applied to a stand-alone PV power system with battery backup. To analyze the operation principle, the proposed FB-TPC topology is redrawn in Fig. 3 the two source ports are connected to a PV source and a battery, respectively, while the output port is connected to a load.

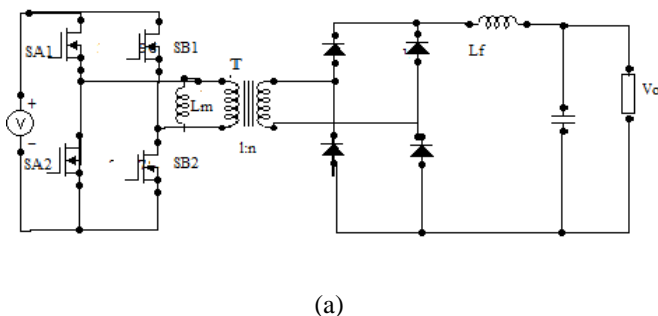
Three power flows in the standalone PV power system are: 1) from PV to load; 2) from PV to battery; and 3) from battery to load. As for the FB-TPC, the input port from the PV source should implement the maximum power tracking to harvest the most energy, while the load port usually has to be tightly regulated to meet the load requirement. Therefore, the mismatch in power between the PV source and load has to be charged into or discharged from the battery port, also two of the three ports should be controlled independently and the third one used for power balance. As a result, two independently controlled variables are necessary.

Ignoring the power loss, we have

$$P_{pv} = p_b + p_o \quad (1)$$

where  $p_{pv}$ ,  $p_b$ , and  $p_o$  are the power flows through the PV, battery, and load port, respectively.

The FB-TPC has three possible operation modes:



- (1) In dual-output (DO) mode, with  $p_{pv} \geq p_o$ , the battery absorbs the surplus solar power and both the load and battery take the power from PV;
- (2) In dual-input (DI) mode, with  $p_{pv} \leq p_o$  and  $p_{pv} > 0$ , the battery discharges to feed the load along with the PV; and
- (3) In single-input single-output (SISO) mode, with  $p_{pv} = 0$ , the battery supplies the load power alone.

When  $p_{pv} = p_o$  exactly, the solar supplies the load power alone and the converter operates in a boundary state of DI and DO modes. This state can either be treated as DI or DO mode.

For simplicity, the following assumptions are made:

1) During the steady state  $C_{pv}$ ,  $C_b$ , and  $C_o$  are large enough and the voltages of the three ports,  $V_{pv}$ ,  $V_b$ , and  $V_o$ , are constant.

2)  $V_{pv} \geq V_b$  case is taken for the switching state analysis. There are four switching states in one switching cycle. The equivalent circuit in each state and key waveforms are shown in the figure 4 and 5 respectively.

**State I [t0 –t1]:**  $S_{A2}$  and  $S_{B2}$  are ON and  $S_{A1}$  and  $S_{B1}$  are OFF, before  $t_0$  while  $i_{Lm}$  freewheels through  $S_{A2}$  and  $S_{B2}$ .  $S_{A1}$  turns ON and  $S_{A2}$  turns OFF at  $t_0$ . Positive voltage is applied across the transformer's primary winding.

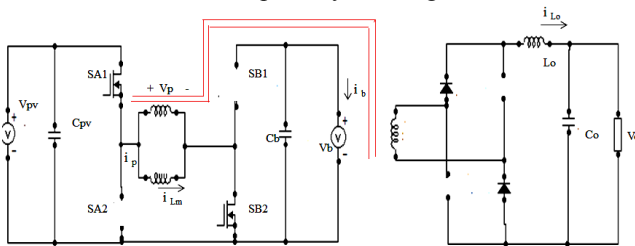


Fig 4(a)-Equivalent circuits of switching state [t0 , t1]

$$\frac{di_{Lm}}{dt} = \frac{V_{pv}}{L_m}$$

$$\frac{di_{Lo}}{dt} = \frac{nV_{pv} - V_o}{L_o}$$

$$i_p = i_{Lm} + ni_{Lo} \tag{2}$$

**State II [t1 –t2]:** At  $t_1$ ,  $S_{B2}$  turns OFF and  $S_{B1}$  turns ON. A positive voltage is applied on the primary winding of the transformer.

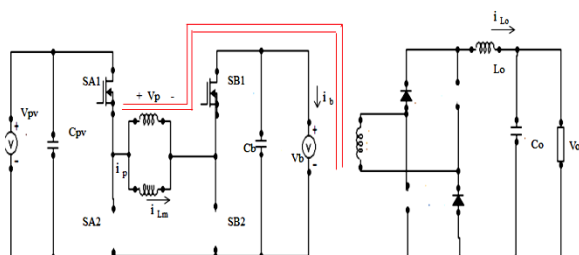


Fig 4(b)-Equivalent circuits of switching state [t1 , t2]

$$\frac{di_{Lm}}{dt} = \frac{V_{pv} - V_b}{L_m}$$

$$\frac{di_{Lo}}{dt} = \frac{n(V_{pv} - V_b) - V_o}{L_o}$$

$$i_p = i_{Lm} + ni_{Lo} \tag{3}$$

**State III [t2 –t3]:**  $S_{A1}$  turns OFF and  $S_{A2}$  turns ON, at  $t_2$ . A negative voltage is applied on the primary winding of the transformer

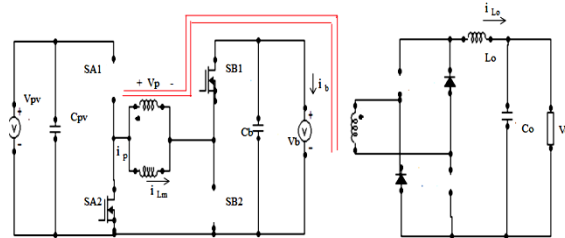


Fig 4(c)-Equivalent circuits of switching state [t2 , t3]

$$\frac{di_{Lm}}{dt} = \frac{-V_b}{L_m}$$

$$\frac{di_{Lo}}{dt} = \frac{nV_b - V_o}{L_o}$$

$$i_p = i_{Lm} - ni_{Lo} \tag{4}$$

**State IV [t3 –t4]:**  $S_{B1}$  turns OFF and  $S_{B2}$  turns ON at  $t_3$ . The  $i_{Lm}$  freewheels through  $S_{A2}$  and  $S_{B1}$  and voltage across the primary winding is clamped at zero

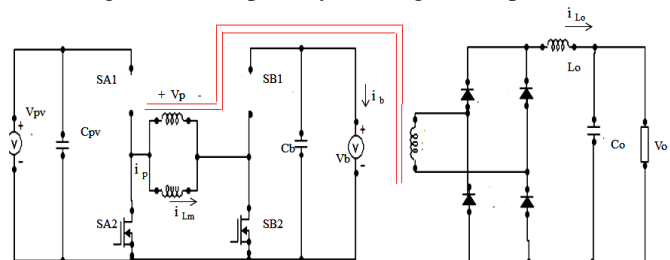


Fig 4(d)-Equivalent circuits of switching state [t3 , t4]

$$\frac{di_{Lm}}{dt} = 0$$

$$\frac{di_{Lo}}{dt} = \frac{-V_o}{L_o}$$

Applying the volt-second balance principle to the magnetizing inductor of the transformer  $L_m$  and the output filter inductor  $L_o$ , respectively, we have:

$$V_{pv} = \frac{D_{B1}}{D_{A1}} V_b$$

$$V_o = n[D_1 V_{pv} + D_2 (V_{pv} - V_b) + D_3 V_b] = 2nD_3 V_b \tag{6}$$

$D_1$ – $D_3$  are the equivalent duty cycles of States I–III, especially,  $D_3$  is the overlapped section of the driven signal

for  $S_{A1}$  and  $S_{B2}$  and  $D_{A1}$  and  $D_{B1}$  are the duty cycles of  $S_{A1}$  and  $S_{B1}$  in the steady state, respectively. For the  $V_{pv} < V_b$  case, the operation principles of the FB-TPC are the same as those of the  $V_{pv} \geq V_b$  case. Differences between these two cases are the voltage applied to the transformer and the direction of the reflected current of  $i_{Lo}$  through primary windings. By following the same analysis, the output voltage  $V_o$  can be given by

$$V_o = n[D_1V_{pv} + D_2(V_b - V_{pv}) + D_3V_b] = 2nD_1V_{pv} \quad (7)$$

The voltage of the PV source  $V_{pv}$  can be regulated with  $D_{A1}$  and  $D_{B1}$  for the maximum power point tracking (MPPT), taking the battery voltage  $V_b$  as constant and the output voltage  $V_o$  can be tightly regulated with  $D_1$  and  $D_3$ .

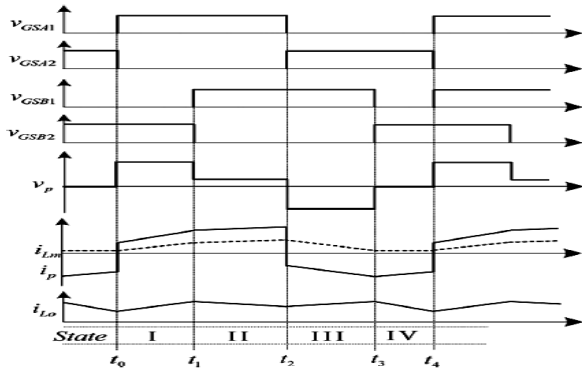


Fig. 5-Key waveforms of the FB-TPC [1]

#### IV. CONTROL STRATEGY

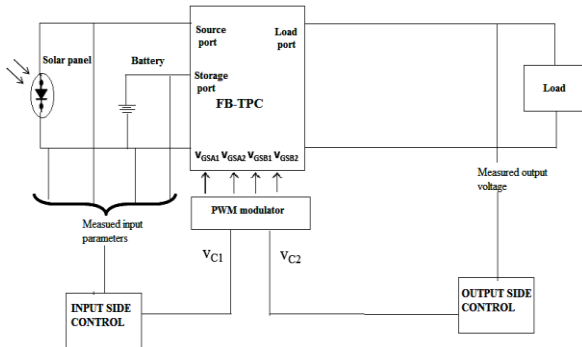


Fig 6-Control diagram for the three port converter

A feedback control structure was used for each operating mode of the converter topology. The objective is to regulate the load voltage and prevent load transitions from affecting the operation of the converter. A multi-loop control scheme was described here. It simultaneously regulates the PV power to achieve the MPPT, or battery charging control and the output voltage. Control diagram of the three port converter is shown in the Fig 6. Multi objective control architecture is implemented to regulate different power ports.

Pulse width modulation scheme can be applied to the proposed FBTPC. Based on the analysis, the proposed PWM scheme and its generation are shown in Fig. 7, where

$V_{tri}$  is the peak-to-peak value of the carrier voltage  $v_{tri}$ , and  $v_{c1}$ ,  $v_{c2}$  are control voltages. In proposed PWM scheme, when  $v_{pv}$  is much higher than  $v_b$ , as shown in Fig. 7, there are only three switching states, states II–IV, in one switching cycle. By regulating the turned OFF time of SA1 with  $v_{c1}$ , the PV power can be controlled to get the MPPT, battery charging control and output voltage  $v_o$  is further controlled with  $v_{c2}$  regulating  $D3$  by adjusting the turned OFF time of SB 1. When  $v_{pv}$  decreases, as shown in Fig. 7, and there are three switching states in one switching cycle, states I–III.

It has two feedback control loops, to generate two control voltages  $v_{c1}$  and  $v_{c2}$  simultaneously. Here a PID controller is used to generate the control voltages.

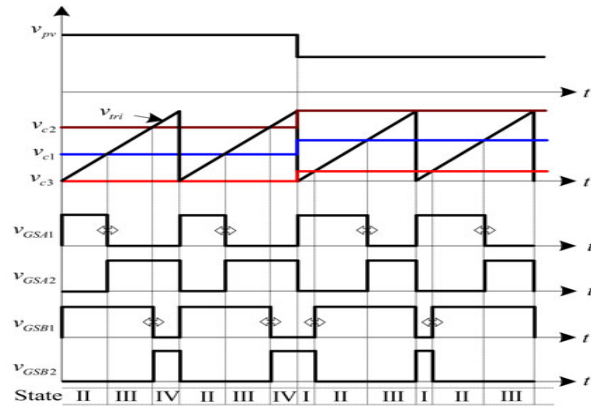


Fig. 7-PWM scheme for the FB-TPC [1].

#### V. SIMULATION RESULTS

The MATLAB 7.12.0(R2011a) is used for the simulation part of the project. MATLAB/Simulink model of the Full Bridge -three port converter with closed loop control is shown in the Figure 8. The PV voltage and battery voltage is adjusted between 38V-76V and 26V-38V respectively. Switching frequency is 100 KHz and load voltage is maintained at 42V.

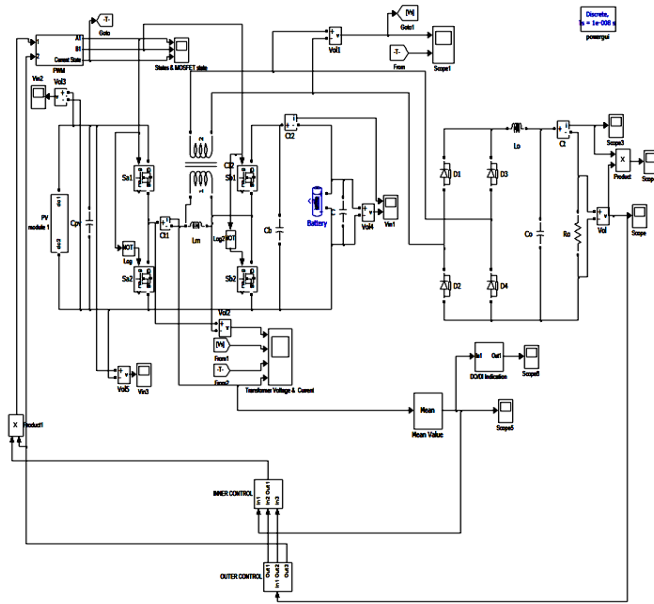


Fig 8-MATLAB/Simulink model of the FB-TPC

The steady-state waveforms of the converter in DO mode with 75V input voltage at full load are given in Fig. 9. The shapes of the corresponding waveforms in DO and DI are the same and the only difference is the average value of the primary winding's current  $i_p$ , and the average value of  $i_p$  is positive in DO mode.

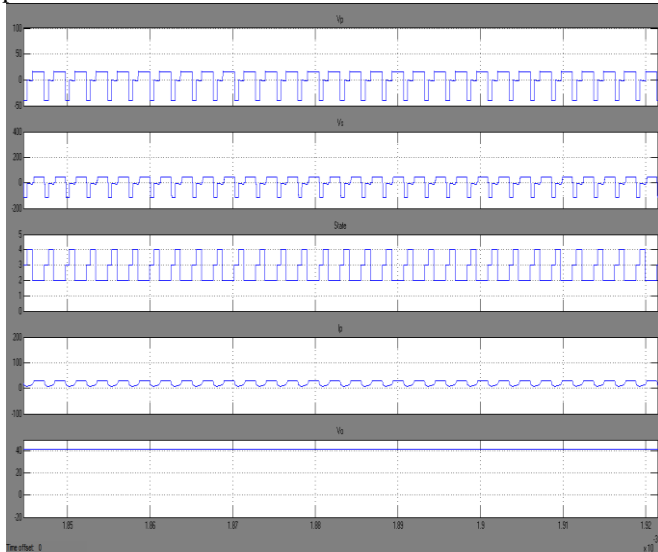


Fig 9- Steady-state waveforms at 75V input voltage with full-load condition

The steady-state waveforms of the converter with 40V input voltage at full load are shown in Fig. 10. Shows the waveforms of the DI mode. The average value of the primary winding's current  $i_p$  is negative.

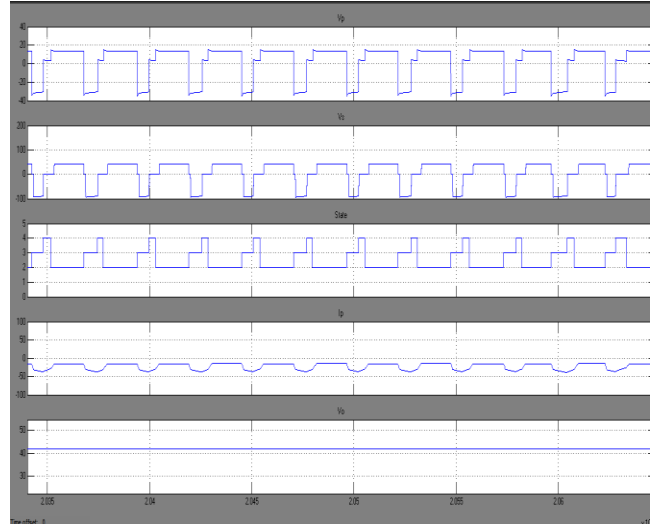
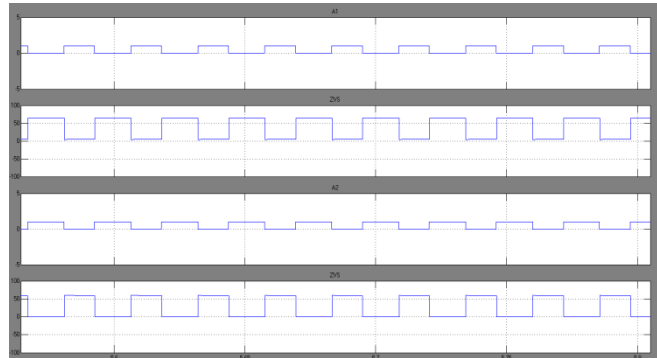
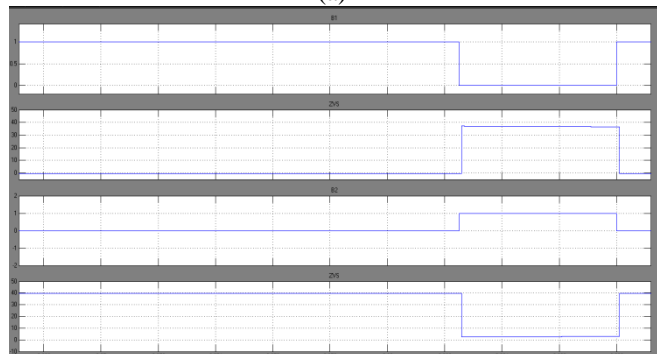


Fig 10-Steady-state waveforms at 40V input voltage with full-load condition

The drain to source voltage and driving voltage on  $S_{A1}$ ,  $S_{A2}$ ,  $S_{B1}$ , and  $S_{B2}$ , in the DO mode at full load, is given in Fig. 11, which indicates that all the switches are turned ON with ZVS. The voltage spike on switches is very small when switches are turned OFF.



(a)



(b)

Fig 11-Driving voltage and drain to source voltage of (a) SA 1 and SA 2 and (b) SB 1 and SB 2 .

Fig.12 gives the transient waveforms with stepping up (from half load to full load) and stepping down (from full load to half load) the resistor load. The load transients occurs at

0.5ms and the output voltage is stable during the load transient.

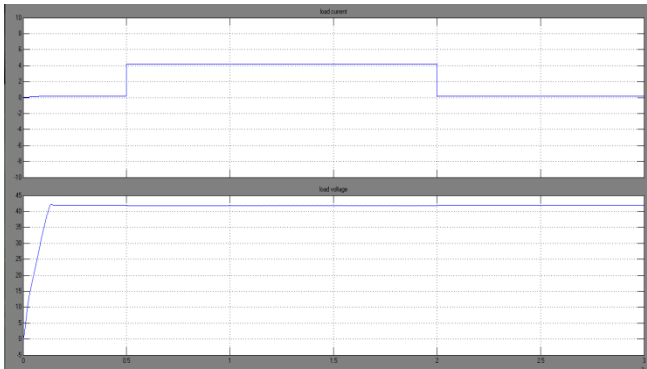


Fig 12-Load transient waveforms by stepping up (half load to full load) and stepping down (full load to half load) load resistors.

The output voltage  $v_o$  is tightly controlled under every mode of operation and load transients.

## VI. CONCLUSION

Alternative electricity generators have a slow dynamic response. Energy storage is therefore necessary to ensure a proper operation of the primary side. A three-port energy management system has been presented here. A systematic method for generating three port converter topologies from full bridge converters and with single-stage power conversion between any two of the three ports has proposed.

Regulate the load voltage and prevent load transitions from affecting the operation of the converter is the control objective. Simulation results validated the effectiveness of the proposed converter. A multi-loop control scheme was described and it has two feedback control loops, simultaneously regulating the PV power to achieve the MPPT and the output voltage.

The proposed converters have benefits of simple topologies and control, reduced number of devices, and a single-stage power conversion between any two of the three ports. They are suitable for renewable power systems with voltages varying over a wide range.

## VII. SCOPE FOR FUTURE STUDY

The application scope of this three-port converter can be extended to power flow control devices and that can be used in residential and commercial buildings, uninterruptible power supplies and high-power automobile applications. The same principle of three port converters can be extended to four-port or multi-port converters. The analysis and control methods and designing for such configurations have to be explored.

## REFERENCES

- [1] Hongfei Wu., Kai Sun, Runruo Chen, Haibing Hu, Member, IEEE, and Yan Xing, "Full-Bridge Three-Port Converters With Wide Input Voltage Range for Renewable Power Systems" IEEE Transactions On Power Electronics, Vol. 27, No. 9, September 2012
- [2] Z. Qian, O. Abdel-Rahman, H. Hu, and I. Batarseh, "An integrated threeport inverter for stand-alone PV applications," presented at the IEEE Energy Convers. Congr. Expo., Atlanta, GA, 2010.
- [3] H. Wu, R. Chen, J. Zhang, Y. Xing, H. Hu, and H. Ge, "A family of threeport half-bridge converters for a stand-alone renewable power system," IEEE Trans. Power Electron., vol. 26, no. 9, pp. 2697–2706, Sep. 2011.
- [4] H. Tao, A. Kotsopoulos, J. L. Duarte, and M. A. M. Hendrix, "Family of multiport bidirectional dc-dc converters," Inst. Electr. Eng. Proc. Elect. Power Appl., vol. 153, no. 15, pp. 451–458, May 2006
- [5] Z. Qian, O. Abdel-Rahman, H. Al-Atrash, and I. Batarseh, "Modeling and control of three-port DC/DC converter interface for satellite applications," IEEE Trans. Power Electron., vol. 25, no. 3, pp. 637–649, Mar. 2010.
- [6] S. Falcones and R. Ayyanar, "Simple control design for a three-port DCDC converter based PV system with energy storage," presented at the IEEE Appl. Power Electron. Conf., Palm Springs, CA, 2010.
- [7] Z. Wang and H. Li, "Integrated MPPT and bidirectional battery charger for PV application using one multiphase interleaved three-port DC-DC converter," in Proc. 26th IEEE Appl. Power Electron. Conf. Expo., 2011, pp. 295–300.
- [8] D. Xu, C. Zhao, and H. Fan, "APWM plus phase-shift control bidirectional dc-dc converter," IEEE Trans. Power Electron., vol. 19, no. 5, pp. 666–675, May 2004
- [9] S. Waffler and J. W. Kolar, "A novel low-loss modulation strategy for high-power bidirectional Buck+Boost converters," IEEE Trans. Power Electron., vol. 24, no. 6, pp. 1589–1599, Jun. 2009.
- [10] A. Kwasinski, "Quantitative evaluation of DC microgrids availability: Effects of system architecture and converter topology design choices," IEEE Trans. Power Electron., vol. 26, no. 3, pp. 835–851, Mar. 2011.
- [11] L. Solero, A. Lidozzi, and J. A. Pomilio, "Design of multiple-input power converter for hybrid vehicles," in Proc. IEEE Applied Power Electronics Conference and Exposition (APEC'04), Anaheim, California, Feb. 2004, pp. 1145–1151.
- [12] H. Tao, J. L. Duarte, and A. M. Marcel, "Three-port triple-half-bridge bidirectional converter with zero-voltage switching," IEEE Trans. Power Electron., vol. 23, no. 2, pp. 782–792, Mar. 2008.
- [13] H. Tao, A. Kotsopoulos, J. L. Duarte, and M. A. M. Hendrix, "Multi-input bidirectional DC-DC converter combining DC-link and magnetic-coupling for fuel cell systems," in Proc. IEEE Industry Application Society Conference and Annual Meeting (IAS'05), Hong Kong, China, Oct. 2005, pp. 2021–2028.
- [14] G. J. Su and F. Z. Peng, "A low cost, triple-voltage bus DC-DC converter for automotive applications," in Proc. IEEE Applied Power Electronics Conference and Exposition (APEC'05), Mar. 2005, pp. 1015–1021
- [15] H. Tao, A. Kotsopoulos, J. Duarte, and M. Hendrix, "Transformer coupled multiport ZVS bidirectional dc-dc converter with wide input range," IEEE Trans. Power Electron., vol. 23, no. 2, pp. 771–781, Mar. 2008.
- [16] Haribaran K, Ned Mohan, "Three-port series-resonant DC-DC converter to interface renewable energy sources with bidirectional load and energy storage ports," IEEE Trans. Power Electron., vol. 24, no. 10, pp. 2289–2297, 2009.
- [17] H. Matsuo, W. Lin, F. Kurokawa, T. Shigemizu, and N. Watanabe, "Characteristics of the multiple-input DC-DC converter," IEEE Trans. Ind. Electron., vol. 51, no. 3, pp. 625–631, June 2004.
- [18] P. Gules, J. D. P. Pacheco, H. L. Hey, and J. Imhoff, "A maximum power point tracking system with parallel connection for PV stand-alone applications," IEEE Trans. Ind. Electron., vol. 55, no. 7, pp. 2674–2683, July 2008.
- [19] H. Al-Atrash and I. Batarseh, "Boost-integrated phase-shift full-bridge converter for three-port interface," in Proc. IEEE PESC, 2007, pp. 2313–2321.
- [20] W. Li, J. Xiao, Y. Zhao and X. He, "PWM plus phase angle shift (PPAS) control scheme for combined multiport DC/DC converters," IEEE Trans. Power Electron., vol. 27, no. 3, pp. 1479–1489, Mar. 2012.